JOURNAL OF AGRICULTURAL AND FOOD CHEMISTRY

Epicatechin Carbonyl-Trapping Reactions in Aqueous Maillard Systems: Identification and Structural Elucidation

VANDANA M. TOTLANI AND DEVIN G. PETERSON*

Department of Food Science, 327 Food Science Building, The Pennsylvania State University, University Park, Pennsylvania 16802-2504

Recently, our group reported via labeling experiments that epicatechin in Maillard reaction aqueous glucose−glycine model systems formed adduct reaction products with C_2, C_3, and C_4 sugar fragments. In the current study, we investigated the identity of the sugar fragment precursors responsible for adduct generation by directly comparing the liquid chromatography−mass spectrometry properties of these reported epicatechin (EC)−sugar fragments adducts with those generated from reactions consisting of only EC and well-known Maillard-generated glucose fragments (i.e., glyoxal, glycolaldehyde, methylglyoxal, glyceraldehyde, etc.). The structural properties of an EC−methylglyoxal adduct reaction product were also analyzed by NMR. The most likely precursors for the C_2, C_3, and C_4 sugar moiety of the EC−sugar fragment adducts were identified as glyoxal, hydroxyacetone, and erythrose, respectively. ^{1}H NMR analysis of the EC−methylglyoxal indicated that the analyte underwent rapid conformational/constitutional exchange. Using cold temperature (−25 °C) two-dimensional NMR analyses (heteronuclear multiple bond coherence, heteronuclear multiple quantum coherence, and ^{1}H−^{1}H correlation spectroscopy), the structure of one of the isomers was reported to consist of a covalent linkage between the C1 position of the methylglyoxal and either the C6 or the C8 position of the EC A ring, presumably generated by hydroxyalkylation and aromatic substitution reactions.

KEYWORDS: Methylglyoxal-epicatechin; epicatechin; carbonyl trapping; glycation; Maillard reaction; flavanol

INTRODUCTION

The Maillard reaction, a carbonyl-amino condensation reaction, is an ubiquitous chemical reaction in life and a well-documented critical food (flavor, color, nutritional value, and toxicity) and biological reaction (aging, inflammation, cardiovascular disease, etc.) (*1*). Recently, our research group has investigated the reactivity of phenolic compounds on the mechanisms of the Maillard reaction. Using ^{13}C-, ^{15}N-labeled glucose (Glu)−glycine (Gly) model Maillard systems, epicatechin (EC) under aqueous conditions was reported to form adduct reaction products with C_2, C_3, and C_4 sugar fragments (*2*), whereas under low moisture roast conditions, EC formed adduct reaction products primarily with C_6 sugar moieties (i.e., 3-deoxyglucosone) (*3*). In both of these previous studies, the addition of EC to Glu−Gly model systems also had a strong inhibitory effect on the generation of Maillard type volatile compounds, which would be anticipated as sugar fragments (i.e., C_2, C_3, and C_4), and deoxyglucosones are known to be key transient precursors of the Maillard reaction (*4*−*7*). Similar results were also reported in model food systems; the addition of EC reduced the generation of Maillard type aroma compounds during thermal processing and/or storage in ultrahigh temperature processed milk (*8*), 0 day and 17 month old spray-dried skim milk powder (*9*), roasted cocoa, and granola bars (*10*).

On the basis of the reported formation of EC−sugar fragmentation adduct reaction products in Maillard model systems (*2*, *3*), it was hypothesized that EC underwent electrophilic aromatic substitution reactions (i.e., hydroxyalkylation) with sugar fragmentation products or known reactive carbonyl compounds [i.e., glyoxal (GO), methylglyoxal (MGO), pyruvaldehyde, glyceraldehyde (GA), dihydroxyacetone (DHA), etc.]. The reactivity of the electron rich phenols with electrophilic carbonyls compounds has been used extensively in the polymer industry for production of phenolic resins (*11*). In food systems, phenolic−carbonyl condensation reactions have been investigated in connection to reduced astringency and increased color development in wine (a low pH system) during the aging process. In particular, condensation reactions between (epi)-catechin and aldehyde contain compounds such as acetaldehyde, glyoxylic acid, furfural, benzaldehyde, etc. and have been reported in wine model systems (*12*−*18*). For the catechin−glyoxylic acid condensation reactions, the C6 and/or C8 position of the flavanol (A ring) and the carbonyl-bearing carbon of the aldehyde compound were reported by NMR to be the bonding sites (*13*). Hashimoto et al. (*19*) also reported a similar flavanol−carbonyl reaction product in oolong tea, 8-C-ascorbyl(−)(−)-epigallocatechin gallate, and suggested the origin of this

* To whom correspondence should be addressed. Tel: 814-865-4525. E-mail: dgp10@psu.edu.

10.1021/jf061244r CCC: $33.50
Published on Web 08/29/2006

Table 1. Aqueous Maillard Model Reactions[a]

	model reactions (mM)																
reactants	1[b]	2[b]	3[b]	4[b,c]	5[b]	6[b,c]	7[b]	8[b]	9[b]	10[b]	11[b]	12[b]	13[b]	14[b]	15[b]	16[b]	17[b]
Glu	10	5															
[$^{13}C_6$]Glu		5															
Gly	10	10															
EC	10	10	10	10	10	10	10	10	10	10	10	10	10	10	10	10	10
acetaldehyde			10														
GO				10										10		10	
glycolaldehyde					10												
MGO						10									10		10
GA							10										
DHA								10									
ACT									10								
2,3-butanedione										10							
3-hydroxyl-2-butanone											10						
D-ERY												10					
E-2-butenal													10				
copper sulfate														10	10		
AA																10	10

[a] Conditions: 125 °C for 30 min (does not include reactor heating time to 125 °C). [b] Fifty milliliters of phosphate buffer (0.1 M, pH 7.0) deionized water. [c] Fifty milliliters of phosphate buffer (0.1 M, pH 8.0) and citrate buffer (0.1 M, pH 5.0).

compound by directly reacting epigallocatechin and dehydroascorbic acid (reactive carbonyl) under slightly basic conditions to generate this flavanol−dehydroascorbate acid adduct.

The radical scavenging property of phenolic compounds has also been previously associated with inhibiting the Maillard reaction in both biological (*20*, *21*) and food model systems (*22*−*24*), although the reaction mechanisms are ill-defined and typically associated with oxidative-dependent Maillard pathways (*25*). The direct reactivity of phenolic compounds, i.e., EC, with key Maillard carbonyl precursors is an alternative mechanism (carbonyl trapping) and may explain in part the previously reported inhibitory effects of phenolic compounds on the Maillard reaction and the large epidemiological data supporting positive health benefits with dietary polyphenolic loads (*26*).

In the current study, the reactivity of EC with select Maillard carbonyl sugar fragmentation products to form EC−sugar fragmentation adduct reaction products was investigated. Identification and structural elucidation of an EC−MGO adduct reaction product were also conducted by liquid chromatography−mass spectrometry (LC-MS) and NMR analysis.

MATERIALS AND METHODS

Chemicals. D-Glu, L-Gly, D-erythrose (ERY), GA, acetaldehyde, hydroxyacetone (ACT), 3-hydroxy-2-butanone, 2,3-butanedione, *E*-2-butenal, D-[$^{13}C_6$]Glu (99% enrichment), methanol-d_4 (99.8% enrichment), and copper sulfate (anhydrous) were obtained from Sigma Aldrich Co. (St. Louis, MO). (−)-EC (≥98% purity) was purchased from Zhejiang Yixin Pharmaceuticals (Beijing, China).

MGO (40% aqueous solution), glycolaldehyde, and DHA were obtained from MP Biomedicals (Aurora, OH). GO (40% aqueous solution) was purchased from Alfa Aesar (Heysham, Lancaster). Sodium citrate trihydrate was purchased from Fischer Scientific. Potassium phosphate, disodium phosphate, hydrochloric acid (6 N), ammonium acetate, citric acid, and high-performance liquid chromatography (HPLC)-grade methanol were obtained from EMD Chemicals (Gibbstown, NJ). Ascorbic acid (AA) and sodium hydroxide were obtained from J.T. Baker (Phillipsburg, NJ). . Phosphate buffer was prepared by dissolving disodium hydrogen phosphate (dibasic) in nanopure water and adjusting the pH to 7 with 1 N HCl. A 0.1 M concentration of citrate buffer was prepared by dissolving citric acid and sodium citrate in nanopure water and adjusting the pH to 5 using 5 M NaOH. The pH of aqueous solution of ammonium acetate solution was adjusted using 1 N HCl solution.

Model Maillard Reaction System. Aqueous reactions were conducted in a heated 600 mL Parr reactor (model 4563, Parr Instrument Co., Moline, IL) under constant stirring (set to 25% speed) at 125 °C for 30 min and subsequently cooled to 20 °C with an internal cooling coil and were immediately prepared for further analyses. All of the reaction mixtures reported in **Table 1** were analyzed at least in duplicate, and for the LC-MS analyses, a representative chromatogram was reported.

Sample Preparation for LC-MS Analysis. A 1 g C_{18} sep-pak cartridge (Supelco, Bellefonte, PA) was preconditioned with methanol (10 mL) and nanopure water (10 mL). An aliquot (10 mL) of the reaction mixture spiked with internal standard butyl paraben (10 μL, 5% solution in methanol) was loaded (1 mL/min) over the preactivated sep-pak cartridge. The cartridge was washed with 10 mL of nanopure water and then eluted with 2 mL of methanol. The isolate was subsequently filtered through 0.45 μm PTFE tip filter (Sigma Aldrich Co.) using a 1 mL syringe (Millipore, Bedford, MA).

LC-MS. Sample analysis was conducted with Shimadzu HPLC system (Shimadzu, Columbia, MD) coupled with Waters ZMD 2000 mass spectrometer (Waters, Milford, MA) via an electrospray ionization probe. The HPLC system consisted of a binary pumping system (LC-10 ADvp), a degasser (DGU-14A), an autosampler (SIL-10vp), a water column heater (TCM model, Waters), a variable wavelength UV/vis detector (λ = 280 nm) (Shimadzu), and a reverse phase C-18 column (4.6 mm × 250 mm, 5 μm packing column, Pursuit C-18 column) (Varian, Inc., Palo Alto, CA). Ten microliter injections of the extracts were separated on a RP-18 column maintained at temperature of 25 °C using a binary solvent system of 10 mM ammonium acetate buffer pH 5 (A) and methanol (B). The mobile phase consisted of a series of linear gradients of B in A starting at 10% B in A (0−2 min), increasing to 80% B in A (2−20 min), then increasing to 99% B in A (21−27 min), and then decreasing to 10% B in A (28−36 min). The effluent was split 1:4 between the electrospray probe (flow rate, 200 μL/min) and the UV/vis detector (flow rate, 800 μL/min) by a postcolumn splitter (zero dead volume T-splitter, Supelco). Mass spectrometric ionization conditions were as follows: desolvation temperature, 250 °C; source temperature, 110 °C; capillary voltage, 3.0 kV; and scan range, *m*/*z* 120−1000 Da.

NMR Sample Preparation/Purification (EC−MGO Adduct). For isolation of EC−MGO analyte, a series of time−temperature reactions (20−125 °C over 0−24 h) were screened to maximize yield/reduce interfering analytes for purification at three different pH conditions (3, 5, and 7), data not shown. The reaction rate for generation of the EC−MGO adduct was kinetically favored at higher pH (*7*); however, the optimal conditions for sample purification were as follows: 10 mM MGO and 10 mM EC were reacted at room temperature in citrate buffer

(75 mL, pH 5) for 1 h under constant stirring. On the basis of LC-MS/UV analysis, four major peaks (>90% of the total peak area of all reaction products) were reported with the MW of 362 $(M - 1)^-$, as well as four minor peaks with a MW of 434 $(M - 1)^-$ and one minor peak with a MW of 634 $(M - 1)^-$. The analytes with a MW of 362, 434, and 634 were considered to be EC−MGO, EC−MGO−MGO adducts, and EC−MGO−EC adducts, respectively. The four MW 362 peaks were termed peaks A−D in accordance with the order of elution; the retention times were 14.69, 15.33, 16.14, and 16.38 min, respectively (as shown in **Figure 5B**). Peak B coeluted with residual EC and therefore was not fractionated. The estimated yield (based on MS peak area of M − 1 ion) was 3.9, 14.1, 10.5, and 19.3% for peaks A−D, respectively.

The reaction mixture was loaded over an activated C-18 sep-pak (50 g Resprep, Restek, Bellefonte, PA) maintaining a flow rate of 1 mL/min. The sep-pak was washed with 25 mL of nanopure water followed by elution with 6 mL of methanol. The methanol extract was concentrated to 1 mL under nitrogen and filtered using a PTFE tip filter (0.45 μm) and a 1 mL syringe. The filtered methanol extract was further fractionated by LC-MS (instrument configuration was the same as described above) utilizing the FractionLynx software (Waters Corp.) and a Waters Fraction Collector (III). The concentrated methanol extracted (10 μL) was injected onto the Pursuit C-18 column maintained at 25 °C using a binary solvent system of 1 mM ammonium acetate buffer (A), pH 5.0, and methanol (B) using a series of linear gradients of B in A starting at 21% B in A (0−16 min), increasing to 23% B in A (16−42 min), then increasing to 90% B in A (42−44 min), and then decreasing to 21% B in A (49−51 min) and held at 21% for 6 min. Three separate isomers were collected over approximately 90 independent injections (triggered on $m/z = 361$), subsequently pooled, frozen at −20 °C, and then freeze-dried in Freezemobile 12 (The Virtis Co, Gardiner, NY) in a two stage process. In the first stage, the HPLC solvent buffer methanol was evaporated until dryness. The white powder obtained was rehydrated with 15 mL of nanopure water, frozen rapidly by immersion in liquid nitrogen, and freeze-dried to yield white powder samples. A small fraction of each isolate was resolublized in methanol and analyzed by LC-MS/UV. Isomers A and D had the highest purity, >96% based on UV peak area, whereas isomer C decomposed during the freeze drying process; purity was <80%. The main decomposition product of each analyte based on LC-MS analysis had an estimated molecular mass of 361 [1 Da lower in MW than the estimated MW 362 $(M - 1)^-$ for the EC−MGO adduct] and likely was a double-charged molecular ion for a EC−MGO adduct dimer. All three isolates were subsequently stored under argon at −20 °C and analyzed by NMR within 2 days of preparation. The NMR signal was poor for analytes A and B (due to the low yield and low purity, respectively); therefore, only the data from peak D were structurally analyzed.

NMR Analysis. The structural configuration of the EC−methyl glyoxal (MGO) was measured by NMR analysis. (−)(−)EC was also analyzed for reference. The isolates/samples (ca. 5−10 mg) were dissolved in 0.6 mL of CD_3OD and flushed with argon gas, and the tube was wrapped with paraffin film. The sample spectra were recorded on a Bruker DRX-400 instrument (Bruker Biospin Co., Billerica, MA), and the chemical shifts (δ values) were referenced to the ^1H or ^{13}C chemical shifts of the internal standard trimethylsilane. ^1H, ^{13}C, gradient-selected $^1H-^1H$ correlation spectroscopy (COSY), gradient-selected heteronuclear multiple quantum coherence (HMQC), and gradient-selected heteronuclear multiple bond coherence (HMBC) spectra were recorded at 400 MHz for ^1H and 100 MHz for ^{13}C. $^1H-^1H$ COSY, HMBC, and HMQC two-dimensional (2D) NMR techniques were used to assign correlations between ^1H and ^{13}C signals. NMR analyses were performed 23 (room temperature) and −25 °C via cryocooling with liquid nitrogen and a temperature controller.

RESULTS AND DISCUSSION

Previously, Totlani and Peterson (*2*) reported that EC generated adduct reaction products with C_2, C_3, and C_4 Glu fragments with the predicted molecular weight (based on $M - 1^-$ pseudoparent ion) of 348 and 622 (C_2 Glu fragment analytes); and 344, 360, 362, 633 (C_3 Glu fragment analytes), and 372

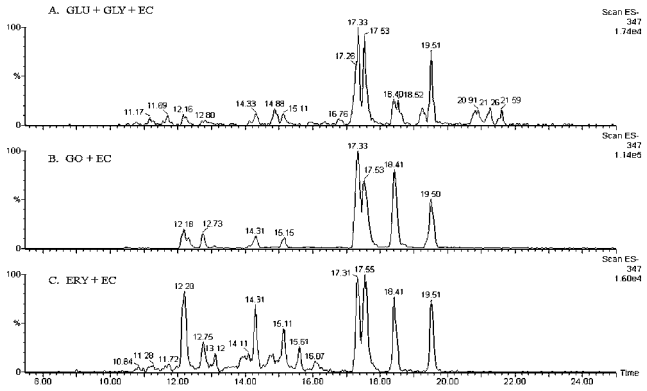

Figure 1. Chromatogram of analyte MW 348 (m/z 347 $[M - 1]^-$) generated from models: (**A**) Glu + Gly + EC, (**B**) GO + EC, and (**C**) ERY + EC. All systems were reacted at pH 7 and 125 °C for 30 min.

(C_4 Glu fragment analyte) in an aqueous Glu plus Gly Maillard reaction model system. To further investigate the identity of the sugar fragment precursors responsible for adduct generation, a series of reactions consisting of EC and well-known Maillard-generated Glu fragments (i.e., GO, glycolaldehyde, MGO, GA, etc.—See **Table 1**) were directly compared to the mass spectral and chromatographic properties of the EC−C_2, −C_3, and −C_4 Glu fragment adducts generated from the Glu, Gly, and EC Maillard reaction systems (model 1, **Table 1**). The identity of the analytes formed in model 1 was also confirmed by direct comparison to model 2 (50% labeled Glu), which was consistent with our previous results, which indicated that the Glu moiety consisted of an intact C_2, C_3, and C_4 Glu fragment (*2*). For all of the EC plus sugar fragment reactions, Gly did not notably influence the formation of EC−sugar fragment adducts (data not shown).

For the EC−C_2 adducts with the predicted MW of 348, only two of the sugar fragments analyzed, GO and ERY, were generated to form this analyte when reacted directly with EC. **Figure 1A−C** illustrates the pseudo-molecular ion $(M - 1)^-$ chromatogram for the EC−C_2 adducts (MW of 348) generated from model 1 (Glu, Gly, and EC), model 4 (GO and EC), and model 12 (ERY and EC) at pH 7. The $M - 1^-$ ion chromatogram or "fingerprint" for model 4 was a good match with model 2 (peak retention times and relative abundance) and consequently suggested that GO (a transient reaction product of Glu−Gly reactions) likely contributed to the formation of this EC−C_2 Glu fragment in the Glu, Gly, and EC system (model 1). The predicted MW of 348 for this reaction product was furthermore supported by the MW of each reactant of 290 and 58 (sum equal to 348) for EC and GO, respectively. It was assumed that ERY, a four-carbon sugar, was undergoing retroaldol cleavage reactions to yield a C_2 fragment (i.e., GO). ERY was proposed by Namiki et al. (*27*) to be formed by a retroaldol cleavage reaction (generate C_2/C_4 fragments) directly from Schiff's base (imine) or prior to Amadori rearrangement.

Interestingly, for the second EC−C_2 Glu fragment product investigated with the predicted MW of 622 (EC dimer + C_2), glycolaldehyde was identified as the sugar fragment reactant (data not shown). Methylmethine-bridged (in the case of acetaldehyde) and carboxymethine-bridged (from glyoxylic acid) epi(catechin) dimers have been documented to form in wine systems by a condensation reaction between two molecules of EC (at C6 or C8 positions—A ring) and acetaldehyde or glyoxylic acid (*12*, *14*, *17*, *18*), and likewise, similar reactions may occur between EC and glycolaldehyde under the reported reaction conditions used for this study (pH 7, 125 °C).

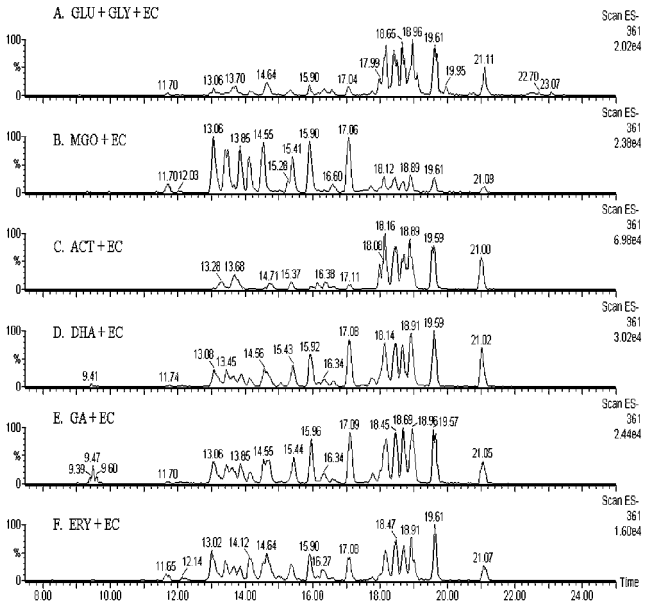

Figure 2. Chromatogram of analyte MW 362 (*m*/*z* 361 [M − 1]$^-$) generated from models: (**A**) Glu + Gly + EC, (**B**) MGO + EC, (**C**) ACT + EC, (**D**) DHA + EC, (**E**) GA + EC, and (**F**) ERY + EC. All systems were reacted at pH 7 and 125 °C for 30 min.

For the generation of the EC−C_3 Glu fragment adducts (MW 344, 360, 362, and 633), ACT, MGO, GAs, DHA, and ERY were all identified as effective C_3 precursors (data only presented for MW 362 analyte; **Figure 2**). The EC−C_3 sugar fragment adducts with the MW of 360 and 344 may have been generated by oxidation and dehydration reactions of the MW 362 analyte or the reactive sugar fragment, respectively. **Figure 2A−F** illustrates the M − 1$^-$ ion chromatogram for the MW 362 EC−C_3 product generated from Glu, Gly, and EC reaction in comparison to MGO−, ACT−, DHA−, GA−, and ERY−EC reactions, respectively, at pH 7. Although each of these five C_3 precursors did generate similar isomers (peaks), ACT had the closest chromatographic "fingerprint" match (relative peak intensity) in comparison to the Glu−Gly system (model 2) and suggested that ACT was likely the primary reactant responsible for the generation of this analyte. Furthermore, in our previous study (*2*), we reported that the addition of EC to a Glu plus Gly reaction dramatically reduced the generation of pyrazine compounds (i.e., 113× for 2,5-dimethylpyrazine); ACT a well known key pyrazine precursor in Maillard reactions (*28*). ERY was considered to undergo retroaldol cleavage to yield the reactive C_3 sugar fragment.

Both GA and DHA were also reported to generate the EC−C_4 sugar fragment analytes (MW 372) as well as ERY (see **Figure 3A−D**). The origin of a four carbon fragment from GA may be explained by retroaldol and aldol reactions. Retroaldol cleavage of the C_1 carbon atom in a GA molecule can result in the generation of formaldehyde (*4*), which can further react with a GA molecule in its enol form (nucleophilic addition) to form a four carbon fragment. Furthermore, GA and DHA can form MGO by a dehydration reaction as a common product; however, the reverse is considered to be not possible under Maillard conditions (*29*). This may explain the similarity in the responses of MGO, GA, and DHA to form three carbon analytes and the inability of MGO to form four carbon fragments adducts with EC. However, on the basis of the isotopomeric analysis of the EC−C_4 sugar fragment (model 2), the sugar moiety was determined to be an intact four carbon fragment, which would exclude GA or DHA and suggested ERY as a likely precursor.

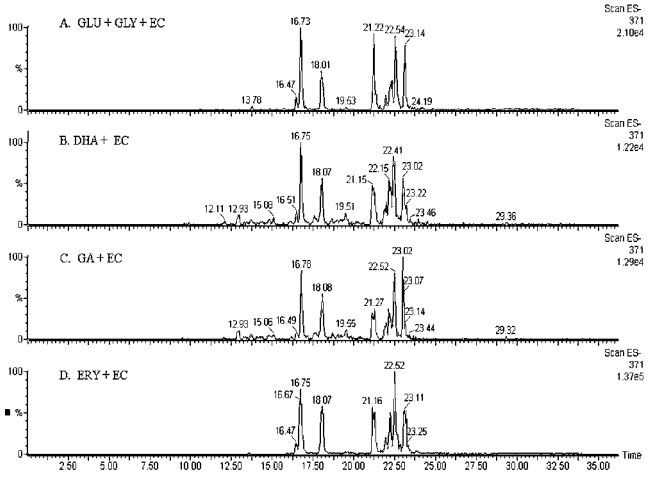

Figure 3. Chromatogram of analyte MW 372 (*m*/*z* 371 [M − 1]$^-$) generated from models: (**A**) Glu + Gly + EC, (**B**) DHA + EC, (**C**) GA + EC, and (**D**) ERY + EC. All systems were reacted at pH 7 and 125 °C for 30 min.

Analysis of the remaining Glu fragments investigated, acetaldehyde, (*E*)-2-butenal, 3-hydroxyl-2-butanone, and 2,3-butanedione, reported negligible or undetectable reactivity with EC to form adducts (data not shown); therefore, these four fragments were not pursued for further analyses.

To gain further insight into the generation of EC−carbonyl sugar fragment adducts in aqueous conditions, the effect of environmental factors, such as the influence of pH (*5*−*8*) and reduction potential (Cu^{2++} or AA) were investigated. The electrophilicity of the carbonyl−sugar fragments would be enhanced at lower pH, whereas at higher pH conditions the proportion of ionized EC would increase [pK_{a1} 8.64 and pK_{a2} 9.41 (*30*)] and thus become more nucleophilic. Furthermore, at higher pH conditions, EC would be more prone to undergo oxidation reactions (phenolate ion has a lower reduction potential vs the protonated phenolic structure) or favor quinone type product generation (alter phenolic reactivity). The estimated reduction potential at pH 7 for EC and AA is 0.57 and 0.27 (*31*), respectively; therefore, AA would be predicted to function as an antioxidant (reducing agent) of EC under these conditions. Copper is a well-known pro-oxidant, presumably due to metal−oxygen complex interactions and/or formation of intermediate oxidation products (i.e., H_2O_2).

Figures 4A−C and **5A−C** illustrate the influence of pH on the generation of the MW 348 and 362 adduct analytes for the GO− and MGO−EC reactions, respectively. For the GO reactions (**Figure 4**) at pH 5, the relative proportion of peaks was altered as eight major peaks corresponding to MW 348 adduct analyte were present instead of four major peaks at neutral pH conditions. The overall intensity of peaks at acidic pH (*5*) was reduced by approximately 50%. For alkaline conditions (pH 8), only two major peaks were generated and the ion intensity decreased by 30%. MGO−EC reactions were similarly influenced by pH. In comparison to pH 7, the ion intensity at pH 5 for major peaks of adduct analyte (MW 362) increased by approximately 200% (enhanced reactivity of reactants), whereas at pH 8, the number of major peaks and the ion intensity for adduct reported did not decrease.

Similar to the noted pH effect, the reduction potential also influenced the generation of GO− and MGO−EC adducts (see **Figures 4E**,**F** and **5E**,**F**). For the GO reactions, addition of copper (oxidizing agent; **Figure 4D**) reduced the ion intensity of the major peaks (retention time, 17.3−19.5 min) by approximately 80% relative to MGO−EC response at pH 7

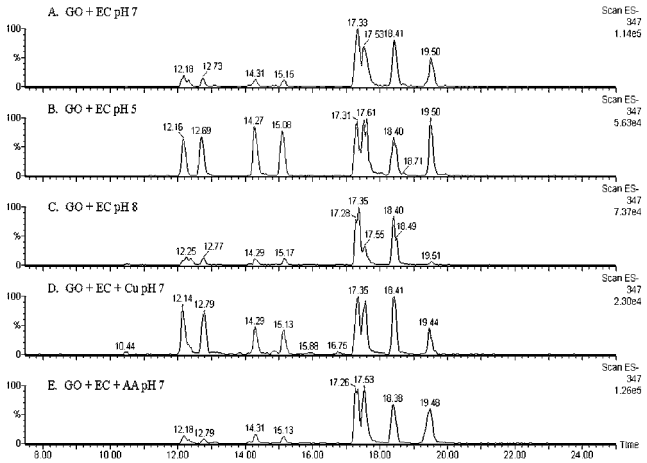

Figure 4. Chromatogram of analyte MW 348 (*m*/*z* 347 [M − 1]$^-$) generated from models: (**A**) GO + EC at pH 7, (**B**) GO + EC at pH 5, (**C**) GO + EC at pH 8, (**D**) GO + EC + copper sulfate (Cu) at pH 7, and (**E**) GO + EC + AA at pH 7. All systems were reacted at 125 °C for 30 min.

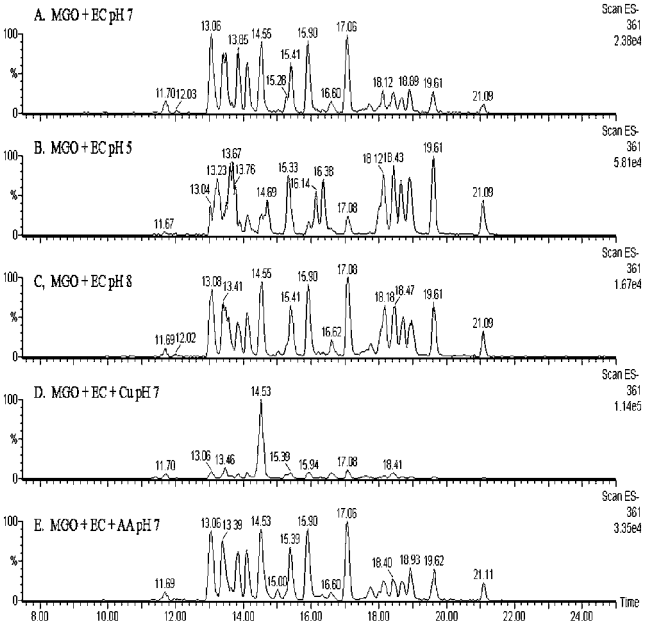

Figure 5. Chromatogram of analyte MW 362 (*m*/*z* 361 [M − 1]$^-$) generated from models: (**A**) MGO + EC at pH 7, (**B**) MGO + EC at pH 5, (**C**) MGO + EC at pH 8, (**D**) MGO + EC + copper sulfate (Cu) at pH 7, and (**E**) MGO + EC + AA at pH 7. All systems were reacted at 125 °C for 30 min.

conditions (**Figure 4A**). The addition of a reducing agent AA (**Figure 4D**) interestingly had no apparent influence on the adduct generation (similar ion chromatogram reported). Flavonoids (i.e., EC) can also chelate trace metals (*32*), which may also explain the reduced reactivity observed. For the methyl−EC reactions, the addition of copper (**Figure 5E**) enhanced the formation of only a single peak or adduct (total ion intensity increased approximately 400%) as compared to the aqueous reaction at pH 7 (**Figure 5A**), whereas the addition of AA (**Figure 5F**) had little impact on adduct generation as its response is similar to a chromatogram reported for pH 7 (**Figure 5A**).

To further examine the mechanisms of EC−carbonyl adduct generation, the structural properties of a purified EC−MGO analyte were analyzed by NMR. The analyte analyzed was the same peak reported in **Figure 5B** with the retention time of 16.38 min (termed peak D). The proton NMR spectra for EC

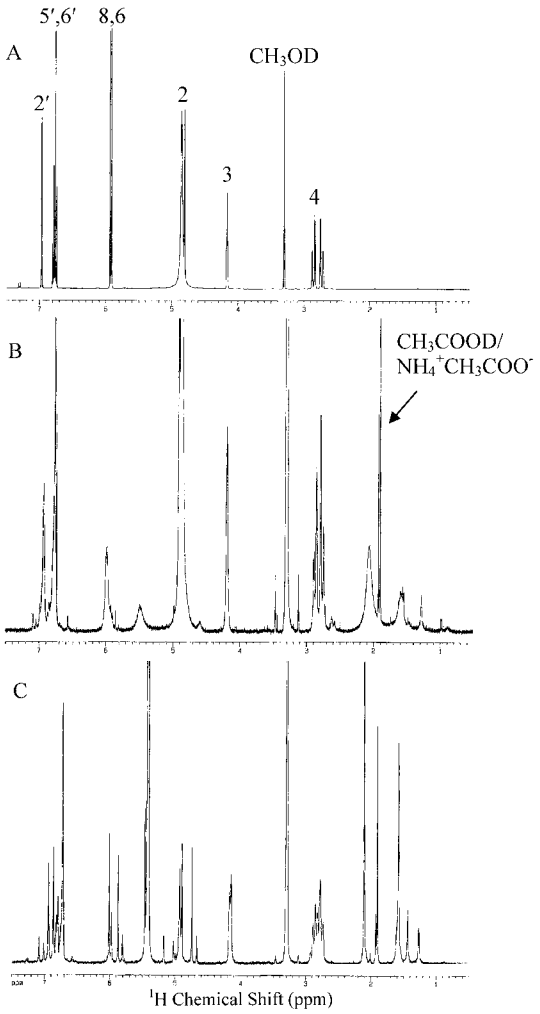

Figure 6. ^{1}H spectra for (**A**) EC at 23 °C, (**B**) EC–MGO adduct peak D at 23 °C, and (**C**) EC–MGO adduct peak D at −25 °C in CD_3OD. In parts **B** and **C**, the two peaks at 1.9 ppm are from AA/ammonium acetate (residual from LC mobile phase buffer).

(as a reference) and the EC−MGO analyte were analyzed at 23 °C (room temperature) and are illustrated in **Figure 6A**,**B**. For **Figure 6A**, the proton assignments are also listed at the top of each peak (refer to **Figure 8A** for carbon assignments). In contrast to the EC proton signal, the signal for the EC−MGO isolate (**Figure 6B**) analyzed at 23 °C reported major "peak broadening", which excluded this data for further structural analysis. The poor spectral properties were considered to be due to one of two possibilities: paramagnetic broadening (free radical) and/or rapid conformational/configurational exchange of the analyte. Furthermore, the analyte was analyzed by LC-MS before and immediately after NMR testing, which suggested that the analyte was of similar high purity at both time points (data not shown). To test the latter mechanism, the sample was analyzed at −25 °C and the proton spectra recorded are illustrated in **Figure 6C**. The EC−MGO isolate under cold NMR conditions reported a dramatic improvement in the proton spectra peak shape (reduced broadening) and confirmed that this analyte was undergoing rapid conformational/configurational exchange. The tabulated ^{1}H spectra from **Figure 6C** are furthermore reported in **Table 2**. The EC sample was also subsequently analyzed by NMR at −25 °C, and the spectrum reported was the same as that illustrated in **Figure 6A** (at 23 °C, data not shown). On the basis of this observation, a series of 2D NMR techniques (HMQC, HMBC, and ^{1}H−^{1}H COSY)

Table 2. ^{1}H NMR Spectral Data for Isomer D in CD_3OD at −25 °C (δ ppm)

7.09, 6.95, 6.87, 6.87, 6.83, 6.80, 6.78, 6.76, 6.75, 6.73, 6.72, 6.01, 5.98, 5.88, 5.81, 5.47, 5.43, 5.19, 4.95, 4.94, 4.92, 4.90, 4.75, 4.67, 4.18, 4.17, 4.15, 2.90, 2.89, 2.86, 2.83, 2.82, 2.81, 2.78, 2.75, 2.74, 1.93, 1.91 1.61, 1.58, 1.44, 1.28, 1.26

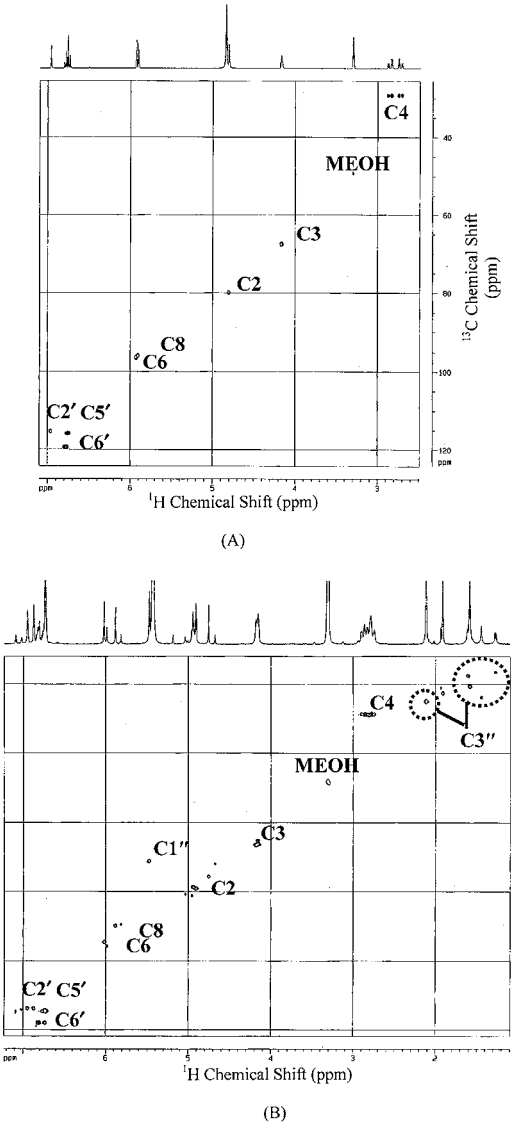

Figure 7. Two-dimensional plots of HMQC for (**A**) EC and (**B**) EC–MGO adduct peak D at –25 °C; carbon assignments are illustrated.

were performed at −25 °C on the EC−MGO isolate; EC was also analyzed for comparison. The HMQC cross-peak correlations (direct ^{1}H→^{13}C coupling) for EC and the EC−MGO isolate are illustrated in **Figure 7A**,**B**, respectively. For **Figure 7A**, the carbon assignments (see **Figure 8A**) are also listed for each cross-peak correlation. Analysis of the H→C correlations for the EC−MGO isolate illustrated strong similarities in the chemical shift across all three rings; however, more correlations were reported within these cross-peak regions (in reference to EC; **Figure 7A**) and may be partially explained by the rapid conformational/configurational exchanges reported for this analyte. This suggested that the MGO moiety of the adduct molecule was altering the chemical environment at all three rings (A−C; see **Figure 8A**). For example, directly comparing the cross-peaks for the B ring assignments (C2′, C5′, and C6′) or the A ring assignments (C6 and C8) between the EC and the EC−MGO adducts, respectively, reported approximately 2× more correlations in these regions. The additional cross-peaks reported in the region of δ16−25 × δ2.1−1.3 (^{13}C × ^{1}H ppm) were consistent with a methyl group or the methyl moiety of MGO. The multiple cross-peaks (five) reported for the methyl group also supported the dynamic nature of this compound.

Table 3. ^{13}C NMR Spectral Data for Isomer D in CD_3OD at −25 °C (δ ppm)[a]

aldehyde or ketone	210.7, 198.7
phenol	166.1, 159.5, 157.7, 156.3, 155.5, 154.5, 153.2, 145.7, 144.9
aromatic or olefinic	130.9, 129.7, 118.0, 116.8, 114.8, 113.9, 111.6, 109.9, 105.3, 104.2, 101.5, 100.1, 99.6, 98.6
aliphatic O–C	79.2, 75.6, 71.8, 71.1, 66.2, 54.3
methyl group	25.0, 22.6, 20.7

[a] On the basis of projection from HMBC analysis.

Careful examination of the HMBC correlations (in addition to the HMQC and ^{1}H−^{1}H COSY) supported the proposed structure for the EC−MGO adduct compound, which is illustrated in **Figure 8Bi** or **8Bii**. The tabulated ^{13}C spectrum (projected from HMBC) is reported in **Table 3**. These structures were "proposed" due to the noted rapid conformational/configurational exchange (**Figure 6**), which prevented a more definitive structural identification or the differentiation of the covalent linkage at the C6 or C8 position on the EC molecule (both of these isomers have a similar chemical environment). The HMBC spectrum showed correlations between δ_C 211.4, δ_C 71.1, and δ_H 2.1 (in combination with the HMQC correlation of δ_C 25.1 and δ_H 2.1; **Figure 7B**) and established the connection between C3″ to C2″ and C1″ (**Figure 8Bi** or **8Bii**). The HMBC spectrum also showed correlations between δ_C 104.7, δ_C 154.5, δ_C 155.4, and δ_H 5.5 (in combination with the HMQC correlation of δ_C 71.1 and δ_H 5.5; **Figure 7B**) and established the connection between C1″ to C6 and C5 and C7 (**Figure 8Bi**) or between C1″ to C8 and C7 and C8a (**Figure 8Bii**).

The ^{1}H−^{1}H COSY spectrum similarly supported the proposed structures and reported correlation between δ_H 2.1 and δ_H 5.5 (linking C3″ to C1″; **Figure 8B**) as well as a "weak" correlation

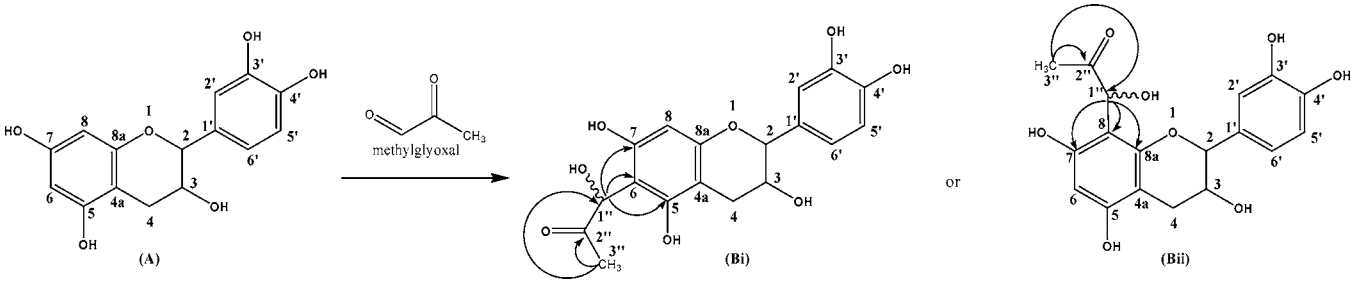

Figure 8. Structure of (**A**) EC and (**B**) proposed EC–MGO adduct peak D illustrating significant HMBC (H→C) correlations.

between δ_H 5.5 and δ_H 6.0 potentially linking C1″ to C8 (**Figure 8Bi**) or C1″ to C6 (**Figure 8Bii**). Furthermore, there were no direct correlations observed between the δ_H peaks at C6 and C8, which would be anticipated due to loss of the hydrogen atom at either of the proposed substituted carbon positions.

On the basis of the structure reported in **Figure 8B**, it was presumed that EC underwent electrophilic aromatic substitution reactions with MGO (or hydroxyalkyation reaction). Electrophilic aromatic substitution reactions involving the A ring of EC for the biogenesis or synthetic generation of EC−(4,8)−EC and EC−(4,6)−EC dimers have been well-documented (*33*, *34*).

The reported rapid conformational/configurational exchange for this analyte (**Figure 6**) was assumed to be due to covalent and/or noncovalent bonding (hydrogen bonding) of the MGO moiety with the EC molecule. The NMR data, as indicated previously, reported at least five different HMQC direct H→C correlations for the methyl group reported and therefore suggested that at least five conformational/constitutional isomeric changes were observed by NMR. On the basis of the structure illustrated in **Figure 8B** and the observed influence of cold temperature conditions on the proton spectrum, keto−enol tautomerization reactions may explain, in part, the multiple isomers reported or the dynamic nature of this reaction product and consequently the analytical challenges encountered for the NMR molecular characterization analyses.

The data presented in this study demonstrate that EC can form covalent bonds with reactive carbonyls such as MGO (function as a carbonyl trapping agent) and provide an alternative mechanism to investigate Maillard chemistry in food and biological systems. The quenching of MGO by EC may also improve our current understanding of the increasing body of epidemiological evidence reporting a positive connection between flavanol-rich foods or beverages (wine/French paradox, cocoa, fruits, and berries) and cardiovascular health (vascular function and platelet reactivity) (*26*). Maillard-derived carbonyl compounds, such as MGO, generated from glycation reactions in vivo (*35*) or from the diet (*35*−*39*) are considered key sources of biological oxidative stress (*40*). For example, MGO has been reported in vascular smooth muscle cells to induce the generation of both reactive oxygen species (H_2O_2, $O_2^{\bullet-}$) and reactive nitrogen species (NO, $ONOO^-$) (*41*). NO is known to regulate numerous biological functions such as reducing platelet activation and adhesion as well as functions such as smooth muscle relaxation (*42*, *43*); however, the corresponding MGO-induced generation of $O_2^{\bullet-}$ inactivates the positive vascular function of NO as NO and $O_2^{\bullet-}$ react to generate $ONOO^-$ (deplete NO). Consequently, a diet-rich in flavanols may relate to lower levels of "carbonyl stress" or a biological state, which promotes cardiovascular health.

The current defined modes of polyphenolic antioxidant activity for health promotion include radical scavenging, metal chelating, and enzyme inhibition (*32*). The ability of EC to form a covalently linked MGO adduct reaction product (remove biological pro-oxidants) may therefore represent an additional or fourth antioxidant mechanism of polyphenolic compounds.

ACKNOWLEDGMENT

We acknowledge the Penn State University NMR center for the use of the NMR instrumentation as well as A. Daniel Jones (Michigan State University) for his insightful comments.

LITERATURE CITED

(1) Mauron, J. The Maillard reaction in foods: A critical review from nutritional standpoint. *Prog. Food Nutr. Sci.* **1981**, *5*, 5−35.
(2) Totlani, V. M.; Peterson, D. G. Reactivity of epicatechin in aqueous glycine and glucose Maillard reaction models: Quenching of C2, C3, and C4 sugar fragments. *J. Agric. Food Chem.* **2005**, *53*, 4130−4135.
(3) Totlani, V.; Peterson, D. G. Epicatechin reactivity in low moisture model systems: Quenching of C5, C6 sugar fragments. In preparation.
(4) Weenan, H.; Tjan, S. B.; Valios, P. J. D.; Bouter, N.; Pos, A.; Vonk, H. Mechanism of pyrazine formation. In *Thermally Generated Flavors: Maillard, Microwave, and Extrusion Processes*; Parliament, T. P., Morello, M. J., McGorrin, R. J., Eds.; American Chemical Society: Washington, DC, 1994; pp 142−157.
(5) Keyhani, A.; Yaylayan, V. Elucidation of the mechanism of pyrazinone formation in glycine model systems using labeled sugars and amino acids. *J. Agric. Food Chem.* **1996**, *44*, 2511−2516.
(6) Weenen, H.; Tjan, S. B. 3-Deoxyglucosone as flavour precursor. In *Trends in Flavour Research*; Maarse, H., v. d. Heij, Eds.; Elsevier Science BV: Amsterdam, London, NewYork, Tokyo, 1994; pp 327−336.
(7) Hollnagel, A.; Kroh, L. W. Formation of alpha dicarbonyl fragments from mono- and disaccharides under caramelization and Maillard reaction conditions. *Z. Lebensm. Unters. Forsch. A* **1998**, *207*, 50−54.
(8) Colahan-Sederstrom, P. M.; Peterson, D. G. Inhibition of key aroma compound generated during ultra-high temperature processing of bovine milk via epicatechin addition. *J. Agric. Food. Chem.* 2005, *53*, 398−402.
(9) Schwambach, S.; Peterson, D. Reduction of stale flavor development in low-heat skim milk powder via epicatechin addition. *J. Agric. Food Chem.* **2005**, *54*, 502−508.
(10) Peterson, D. G.; Totlani, V. A. Influence of flavonoids on the thermal generation of aroma compounds. In *Phenolics in Foods and Natural Health Products*; ACS Symposium Series 909; American Chemical Society: Washington, DC, 2005; pp 143−160.
(11) Shafizadesh, J. E.; Guionnet, S.; Tillman, M. S.; Seferis, J. C. Synthesis and characterization of phenolic resole resins for composite application. *J. Appl. Polym. Sci.* **1998**, *73*, 505−514.
(12) Timberlake, C. F.; Bridle, P. Interactions between anthocyanins, phenolic compounds, and acetaldehyde and their significance in red wine. *Am. J. Enol. Vitic.* **1976**, *27*.
(13) Es-Safi, N.; Guerneve, C.; Cheynier, V.; Moutounet, M. New phenolic compounds obtained by evolution of (+)-catechin and glyoxylic acid in hydroalcoholic medium. *Tetrahedron Lett.* **2000**, *40*, 1917−1921.
(14) Pissarra, J.; Mateus, N.; Rivas-Gonzalo, J.; Buelga, S. C.; De Freitas, V. Reaction between malvidin 3-glucoside and (+)-catechin in model solutions containing different aldehydes. *J. Food Sci.* **2003**, *68*, 478−481.
(15) Es-Safi, N.; Cheynier, V.; Moutounet, M. Study of the reactions between (+)-catechin and furfural derivatives in the presence or absence of anthocyanins and their implication in food color change. *J. Agric. Food Chem.* **2000**, *48*, 5946−5954.
(16) Fulcrand, H.; Doco, Y.; Es-Safi, N.; Cheynier, V.; Moutounet, M. Study of the acetaldehyde induced polymerisation of flavan-3-ols by liquid chromatography-ion spray mass spectrometry. *J. Chromatogr. A* **1996**, *752*, 85−91.
(17) Saucier, C.; Bourgeois, G.; Vitry, C.; Roux, D.; Glories, Y. Characterization of (+)-catechin-acetaldehyde polymers: A model for colloidal state of wine polyphenols. *J. Agric. Food Chem.* **1997**, *45*, 1045−1049.
(18) Es-Safi, N.-E.; Fulchrand, H.; Cheynier, V.; Moutounet, M. Competition between (+)(-)catechin and (-)(-)epicatechin in acetaldehyde-induced polymerization of flavanols. *J. Agric. Food Chem.* **1999**, *47*, 2088−2095.

(19) Hashimoto, F.; Nonaka, G.; Nishioka, I. Tannins and related compounds. XC. 8-ascorbyl (-)(-)epigallocatechin 3-O-gallate, from oolong tea. *Chem. Pharm. Bull.* **1989**, *37*, 3255−3263.
(20) Matsuura, N.; Aradati, T.; Sasaki, C.; Kojima, H.; Ohara, M.; Hasegawa, J.; Ubukata, M. Screening system for the Maillard reaction inhibitor from natural product extract. *J. Health Sci.* **2002**, *48*, 520−526.
(21) Wu, C.-H.; Yen, G.-C. Inhibitory effect of naturally occuring flavonoids on the formation of advanced glycation endproducts. *J. Agric. Food Chem.* **2005**, *53*, 3167.
(22) Wang, Y. Effects of naturally occurring phenolic compounds on the formation of Maillard aromas. Ph.D. dissertation, Rutgers State University, 2000.
(23) D'Agostina, A.; Negroni, M.; Arnoldi, A. Autoxidation in the formation of volatiles from glucose-lysine. *J. Agric. Food Chem.* **1998**, *46*, 2554−2559.
(24) Arnoldi, A.; Corain, E. Effects of free radicals on pyrazine formation in the Maillard reaction. In *Flavour Science. Recent Developments*; Taylor, A. J., Mottram, D. S., Eds.; The Royal Society of Chemistry: Cambridge, United Kingdom, 1996; pp 217−220.
(25) Nagasawa, T.; Tabata, N.; Ito, Y.; Nishizawa, N.; Aiba, Y.; Kitts, D. Inhibition of glycation reaction in tissue protein incubations by water soluble rutin derivative. *Mol. Cell Biochem.* **2003**, *249*, 3−10.
(26) Graf, B. A.; Milbury, P. E.; Blumberg, J. P. Flavonols, flavones, flavanones, and human health: Epidemiological evidence. *J. Med. Food* **2005**, *8*, 281−290.
(27) Hayashi, T.; Namiki, M. Formation of two-carbon fragment at an early stage of the browning reaction of sugar with amine. *Agric. Biol. Chem.* **1980**, *44*, 2575−2580.
(28) Weenan, H.; Tjan, S. B. 3-Deoxyglucosone as flavour precursor. *Trends in Flavour Research*; Weurman Flavour Research Symposium; Elsevier: Noordwijkerhout, 1994; pp 327−338.
(29) Kabyemela, B. M.; Adschiri, T.; Malaluan, R.; Arai, K. Degradation kinetics of dihydroxyacetone and glyceraldehyde in subcritical and supercritical Water. *Ind. Eng. Chem. Res.* **1997**, *36*, 2025−2030.
(30) Jovanovic, S.; Hara, Y.; Steenken, S.; Simic, M. G. Antioxidant potential of gallocatechin. A pulse radiolysis and laser photolysis study. *J. Am. Chem. Soc.* **1995**, *117*.
(31) Jovanovic, S.; Simic, M. G. Antioxidants in nutrition. *Ann N. Y. Acad. Sci.* **2000**, *899*, 326−334.
(32) Pietta, P.-G. Flavonoids as antioxidants. *J. Nat. Prod.* **2000**, *63*, 1035−1042.
(33) Saito, A.; Doi, Y.; Tanaka, A.; Matsuura, N.; Ubukata, M.; Nakajima, N. Systematic synthesis of four epicatechin series procyanidin trimers and their inhibitory activity on the Maillard reaction and antioxidant activity. *Bioorg. Med. Chem.* **2004**, *12*, 4783−4790.
(34) Balas, L.; Vercauteren, J. Extensive high-resolution reverse 2D-NMR analysis for the structural elucidation of procyanidin oligomers. *Magn. Reson. Chem.* **1994**, *32*, 386−393.
(35) Baynes, J.; Monnier, V.; Ames, J.; Thorpe, S. The Maillard reaction: Chemistry at the interface of nutrition, aging, and disease. In *8th International Symposium on the Maillard Reaction*; Baynes, J., Monnier, V., Ames, J., Thorpe, S., Eds.; Annals of the New York Academy of Science: Charleston, SC, 2004; p 954.
(36) Cai, W.; Gao, Q. D.; Zhu, L.; Peppa, M.; He, C.; Vlassara, H. Oxidative stress-inducing carbonyl compounds from common foods: Novel mediators of cellular dysfunction. *Mol. Med.* **2002**, *8*, 337−346.
(37) Vlassara, H.; Cai, W.; Crandall, J.; Goldberg, T.; Oberstein, R.; Dardaine, V.; et al. Inflammatory mediators are induced bydietary glycotoxins, a major risk factor for diabetic angiopathy. *Proc. Natl. Acad. Sci. U.S.A.* **2002**, *99*, 15596−15601.
(38) Uribarri, J.; Peppa, M.; Cai, W.; Goldberg, T.; Lu, M.; He, C.; et al. Restriction of dietary glycotoxins reduces excessive advanced glycation end products in renal failure patients. *J. Am. Soc. Nephrol.* **2003**, *14*, 728−731.
(39) Koschinsky, T.; He, C. J.; Mitsuhashi, T.; Bucala, R.; Liu, C.; Buenting, C.; Heitmann, K.; Vlassara, H. Orally absorbed reactive glycation products (glycotoxins): An environmental risk factor in diabetic nephropathy. *Proc. Natl. Acad. Sci. U.S.A.* **1997**, *94*, 6474−6479.
(40) Rahbar, S.; Figarola, J. L. Novel inhibitors of advanced glycation endproducts. *Arch. Biochem. Biophys.* **2003**, *419*, 63−79.
(41) Chang, T.; Wang, R.; Wu, L. Methylglyoxal-induced nitric oxide and peroxynitrite production in vascular smooth muscle cells. *Free Radical Biol. Med.* **2005**, *38*, 286−293.
(42) Furchgott, R. F.; Zawadzki, J. V. The obligatory role of endothelial cells in the relaxation of arterial smooth muscle by acetylcholine. *Nature* **1980**, *288*, 373−376.
(43) Radomski, M. W.; Palmer, R. M.; Moncada, S. The role of nitric oxide adn cGMP in platelet adhesion to vascular endothelium. *Biochem. Biophys. Res. Commun.* **1987**, *148*, 1482−1489.

Received for review May 3, 2006. Revised manuscript received July 11, 2006. Accepted July 14, 2006. The project was supported by the National Research Initiative of the U.S. Department of Agriculture Cooperative State Research, Education and Extension Service, Grant 2004-35503-14794.

JF061244R